

Effects of recombinant human endostatin and its synergy with cisplatin on circulating endothelial cells and tumor vascular normalization in A549 xenograft murine model

Na Li · Dawei Zheng · Xiyin Wei · Ziliang Jin ·
Cuicui Zhang · Kai Li

Received: 7 February 2012 / Accepted: 24 February 2012 / Published online: 10 March 2012
© Springer-Verlag 2012

Abstract

Purpose Endostatin can normalize the tumor vasculature to some extent. However, exact length of its time window and corresponding markers for tumor vascular normalization are needed to be explored.

Methods The A549 lung adenocarcinoma xenograft murine model was treated with recombinant human endostatin (rh-endostatin) for 14 days. Cisplatin was combined in different schedules. The effects of rh-endostatin on circulating endothelial cells (CECs) by flow cytometry, tumor vasculature and angiogenesis-related factors by confocal microscope and immunohistochemistry, and anti-tumor efficacy of cytotoxic drugs were observed.

Results The activated CECs (aCECs) were increased on day 7 and decreased on day 10, and apoptotic CECs were increased on day 10. Tumor vasculature was transiently normalized with increased collagen coverage, decreased vessel permeability, intratumoral hypoxia, and microvascular density from day 7 to 10 after rh-endostatin administration. Extracellular matrix metalloproteinase inducer, vascular endothelial growth factor, matrix metalloproteinase (MMP)-2, and MMP-9 were transiently decreased by rh-endostatin from day 4 to 10, whereas the opposite effects

were observed with tissue inhibitors of matrix metalloproteinase (TIMP)-1 and TIMP-2. The maximal anti-tumor effects of cisplatin were observed on administration from day 5 to 9 after rh-endostatin initial administration.

Conclusions Rh-endostatin could transiently normalize tumor vasculature, probably via regulation of both pro- and anti-angiogenesis factors. The synergistic efficacy of anti-angiogenesis and chemotherapy was found during “the normalization window”. CEC could be a feasible blood biomarker for defining “vascular normalization window” and providing the evidence to make an optimizing combination therapeutic schedule in human tumor.

Keywords Rh-endostatin · Vascular normalization · Circulating endothelial cells · Matrix metalloproteinases · Collagen coverage of tumor vessels

Abbreviations

Rh-endostatin	Recombinant human endostatin
NSCLC	Non-small-cell lung cancer
VEGF	Vascular endothelial growth factor
MMP	Matrix metalloproteinase
TIMP	Tissue inhibitors of matrix metalloproteinase
EMMPRIN	Extracellular matrix metalloproteinase inducer
PB	Peripheral blood
FC	Flow cytometry
CECs	Circulating endothelial cells
aCECs	Activated circulating endothelial cells
HIF-1 α	Hypoxia-inducible factor-1 α
MVD	Microvascular density
IFP	Interstitial fluid pressure
EPCs	Endothelial precursor cells
IOD	Integrated optical density

N. Li · X. Wei · Z. Jin · C. Zhang · K. Li (✉)
Department of Thoracic Oncology, Key Laboratory of Cancer Prevention and Therapy, Lung Cancer Center of Tianjin, Cancer Hospital of Tianjin Medical University, Tianjin, China
e-mail: likai5@medmail.com.cn

N. Li
Department of Oncology, The People's Hospital of Rushan,
Weihai 264500, Shandong Province, China

D. Zheng
Department of Cardiology, The People's Hospital of Rushan,
Weihai 264500, Shandong Province, China

ECM	Extracellular matrix
TAF	Tumor angiogenesis factor

Introduction

In 1971, Judah Folkman (1971) first proposed that tumor growth and metastasis were dependent on blood vasculature, which means that blocking angiogenesis could be an effective strategy to arrest tumor growth. Studies on anti-angiogenesis have since rapidly expanded.

The conventional rationale of anti-angiogenesis therapy was that suppression of angiogenesis and blood supply could cause tumor death through “starvation”. However, the concept of “vascular normalization”, proposed by Jain (2005), provided another explanation. Jain hypothesized that anti-angiogenesis actually “normalizes” tumor vasculature and transiently increases blood perfusion within the tumor and alleviates hypoxia, thus, enhancing the delivery of oxygen and drugs to tumor cells to increase the malignancies response to chemotherapy. Based on his hypothesis, synergistical depression of tumor growth should be achieved when chemotherapy is given during normalization window. However, according to other observations, vascular normalization was transient and reversible (only about 1 week by report) (Batchelor et al. 2007). The markers are, thus, particularly important for monitoring the normalization period. Unfortunately, there have been no powerful biomarkers to help define the duration of the window and the optimal administration schedule.

Rh-endostatin, a refolding and modified recombinant human endostatin that acts specifically on neovascular endothelial cells, has been proven effective to combine with chemotherapy on patients with advanced non-small-cell lung cancer (NSCLC) (Wang et al. 2005). Based on results from clinical trials, it was approved for NSCLC by the State Food and Drug Administration of China in 2005. In the present study, the effects of rh-endostatin on pro- and anti-angiogenesis factors, variations of amounts of CECs, and tumor vasculature were desirably observed and thus enabling the exploration of the markers that correspond with the “normalization window” and investigating the optimizing schedule of combination therapies through the comparison of tumor growth inhibition by cisplatin prior to normalization and inside this window.

Materials and methods

Cell culture and animal model

Female Balb/c nude mice (4 or 5 weeks old, weighing between 16 and 18 g) were purchased from Vitalriver

(Beijing, China) and maintained under specified pathogen-free conditions in the Animal Experimental Center at the Key Laboratory of Cancer Prevention and Therapy (Tianjin, China). The animals had free access to food and water. Human lung adenocarcinoma A549 cell line, purchased from cell bank of Chinese Academy of Sciences, was incubated in RPMI-1640 medium containing 10 % fetal bovine serum at 37 °C in a humidified atmosphere of 5 % CO₂.

Reagents and drugs

Rh-endostatin was cordially provided by Simcere Pharmaceutical Group (Jiangsu, China). Cisplatin was purchased from Biovalley Biotechnology (Yuannan, China). CD105-FITC and its isotype control, CD45-PECY5 and its isotype control, Annexin V-FITC, and propidium iodide (PI) were exclusively purchased from eBioscience Company (San Diego, CA, USA). CD146-PE and its isotype control were purchased from Biologend Company (San Diego, CA, USA). TRITC-dextran and FITC-lectin were purchased from Sigma-Aldrich Company (St. Louis, MO, USA). Anti-CD34 antibody (1:10, rat monoclonal), anti-VEGF antibody (1:75, mouse monoclonal), anti-hypoxia-inducible factor-1 α (HIF-1 α) antibody (1:100, mouse monoclonal), anti-EMMPRIN antibody (1:100, mouse monoclonal), anti-TIMP-1 antibody (1:100, mouse monoclonal), and anti-TIMP-2 antibody (1:100, mouse monoclonal) were purchased from Abcam (Cambridge, MA, UK). Anti-MMP-2 antibody (1:10, goat polyclonal) and anti-MMP-9 antibody (1:10, goat polyclonal) were purchased from R&D Company (Minneapolis, MN, USA). PV kits and DAB kits were purchased from Zhongshanjinqiao Company (Beijing, China). Masson’s Trichrome Staining was purchased from Fuzhoumaixin Company (Fujian, China).

Animal model and treatment protocol

A549 cells in exponential growth phase were treated with pancreatin–EDTA and resuspended in PBS. The athymic mice were subcutaneously injected with 10⁷ cells per mouse into the left flank. The tumor-bearing mice were randomly and equally divided into three groups for mono-drug therapy (each group with 48 mice) when the tumors reached 100 mm³. Mice in control group were subcutaneously injected with 0.2 ml 0.9 % normal saline for 14 days, whereas mice in rh-endostatin group were subcutaneously injected with 20 mg kg⁻¹ day⁻¹ rh-endostatin for 14 days. Mice in cisplatin group were intraperitoneally injected with 4 mg kg⁻¹ day⁻¹ cisplatin for 5 days.

Five mice from each group were killed on days 1, 4, 7, 10, 16, and 22 from the initiation of treatment, respectively,

to harvest tumor tissues for immunohistochemistry analyses and blood samples for flow cytometry (FC) analyses. Another three mice from each group for each of the six time points were intravenously injected with rhodamine-conjugated dextran and FITC-lectin and killed to observe the vasculature morphology and vascular permeability.

Based on the results of the mono-drug therapy experiment, a combined treatment protocol to investigate the optimal therapeutic administration schedule was established. The transplantation tumor models were established by the previous methods. The tumor-bearing animals were randomly and equally divided into four groups (each group with 30 mice) when the tumors reached 100 mm³. Mice in control group were subcutaneously injected and intraperitoneally injected with 0.2 ml 0.9 % normal saline for 14 days. Mice in combined group 1 were subcutaneously injected with 20 mg kg⁻¹ day⁻¹ rh-endostatin for 14 days and intraperitoneally injected with 4 mg kg⁻¹ day⁻¹ cisplatin on days one to five. Mice in combined group 2 were subcutaneously injected with 20 mg kg⁻¹ day⁻¹ rh-endostatin for 14 days and intraperitoneally injected with 4 mg kg⁻¹ day⁻¹ cisplatin on days five to nine. Mice in combined group 3 were intraperitoneally injected with 4 mg kg⁻¹ day⁻¹ cisplatin on days one to five and subcutaneously injected with 20 mg kg⁻¹ day⁻¹ rh-endostatin on days six to nineteen.

Tumor volumes were measured with digital caliper every 3 days and calculated by the formula $0.52 \times \text{length} \times \text{width}^2$. The growth increment of tumor (Vd) was defined as the value of the measured volume of tumor (V) minus that of before treatment (V0). Tumor volume inhibition rate (%) was obtained as $(1 - \text{tumor volume of treatment group/tumor volume of control group}) \times 100 \%$. The tumor growth curve was drawn after treatment.

All the animal experiments conducted in the current research were in accordance with guidelines approved by the Institute Animal Care and Use Committee of Cancer Hospital of Tianjin Medical University.

Measurement of CEC number and viability by flow cytometry

CECs in the PB were enumerated by four-color FC using a panel of monoclonal antibodies reacting with murine CD45 (to exclude hematopoietic cells). Many markers have been used to identify CECs because of the diversity of their origin and complexity of their differentiation. The currently recognized markers are CD45⁻CD146⁺Flk1⁺ (Beaudry et al. 2005). In addition, Mancuso et al. (2001) chose CD105 to distinguish activated CECs (aCECs) from total cells. Given that mature endothelial cells (negative for CD45) are viable and continue to exhibit proliferative capacity, despite their terminal differentiation (Beaudry et al. 2005),

CD45⁻CD146⁺CD105⁺ was used to identify aCECs in accordance with the literature (Mancuso et al. 2001), and apoptotic CECs were defined as CD45⁻CD146⁺Annexin V⁺PI⁻ (Khan et al. 2005). Approximately 100 μl of PB was collected in each EDTA tube. Tube 1 was added with 10 μl each of PECY5, PE, and FITC isotype control antibody. Tube 2 was added with 10 μl each of CD45-PECY5 and CD146-PE. Tube 3 was added with 10 μl each of CD45-PECY5, CD146-PE, and CD105-FITC. After 30 min of incubation at room temperature in the dark, the red cells were lysed with PBS, and tubes 1 and 3 were resuspended for analyses. Approximately 5 μl of Annexin V-FITC was added into tube 2 and then incubated for 15 min at room temperature in the dark. The cells were washed with binding buffer, and 5 μl of PI was added. Cell suspensions were evaluated using a FACSCalibur (Beckman Coulter, CA, USA). After acquisition of at least 100,000 cells per sample, analyses were considered as informative when adequate numbers of events (i.e., >100, typically 300–400 events) were collected in the CEC enumeration gates.

Fluorescence microscopy assay

High molecular weight tracers, such as TRITC-dextran (155 kDa), were used to detect and measure the permeability and integrity of tumor blood vessels, and vasculatures were represented by probe molecules, such as FITC-lectin, which could be attached to vessel walls (Huang et al. 2009). Briefly, 100 μl of 50 mg/kg TRITC-dextran was injected intravenously and allowed to circulate for 3 h, and thereafter, 100 μl of 10 mg/kg FITC-lectin was injected intravenously through tail vein of each mouse. Mice were killed after 10 min, and tumor tissues were cryosectioned (4 μm thick) and examined via fluorescence microscopy. Images were captured using an Olympus fluorescence microscope in five random fields at 400× magnification. Image Pro Plus 6.0 was used to calculate vascular permeability (the area of diffused TRITC-dextran/the total area × 100 %).

Immunohistochemistry

Paraffin-embedded tumor tissues were immunohistochemically stained with indicated primary antibodies and streptavidin-conjugated horseradish peroxidase (HRP) secondary antibodies as described previously (Al-Dissi et al. 2010). PBS was replaced with a primary antibody to serve as negative control.

Integrated optical density (IOD) assay

Different images were semi-quantitated for each marker in each tumor sample by measuring the pixel area of the

positive staining of individual markers in 10 random fields at 400× magnification. Image Pro Plus 6.0 software was used to calculate the IOD of each image to detect the protein level.

Microvascular density (MVD)

MVD was independently assessed according to the Weidner method by two observers (1995). Collagen around the tumor vessels was stained blue by Masson's trichrome staining. The images of the co-localization of CD34 and collagen were calculated in 10 random fields at 400× magnification, and the percentages of vessels surrounded by more than 50 % collagen were calculated to determine the ratio of collagen covered vessels, which manifested the vascular maturity as reported by Huang and Chen (2010).

Statistical analysis

Statistical analysis was performed using SPSS 16.0 software. Measurement data were expressed as mean ± SD. Statistical significance was determined by one-way ANOVA. LSD was applied for multiple means comparisons in regular variance, and Dunnett's T3 was used for multiple means comparisons in irregular variance. The correlation among the indexes was assessed by Spearman rank correlation coefficient. Statistical significance was established at $P < 0.05$.

Results

Inhibitory effects of rh-endostatin combined with cisplatin on transplanted A549 tumors

The growth increment of tumor in different groups was exhibited as follows: for rh-endostatin group $V_d = (182.408 \pm 46.379) \text{ mm}^3$, the tumor volume inhibition rate was 28.67 %, for cisplatin group $V_d = (234.774 \pm 59.588) \text{ mm}^3$, the tumor volume inhibition rate was 16.72 %, and for control group $V_d = (288.802 \pm 66.497) \text{ mm}^3$. A significant difference between rh-endostatin and control group was found ($P = 0.013$), whereas there was no significant difference between cisplatin and control group ($P = 0.167$). All the three combined therapy groups significantly inhibited the tumor growth compared with control group ($P = 0.010$, $P = 0.000$, and $P = 0.000$, respectively). The growth increments of tumors were (462.48 ± 128.85) , (268.28 ± 83.97) , (404.65 ± 117.66) , and $(677.75 \pm 102.80) \text{ mm}^3$ in combined group 1, combined group 2, combined group 3, and control group, respectively. The tumor volume inhibition rates were

31.69, 53.26, and 35.46 % in combined group 1, combined group 2, and combined group 3, respectively. The growth curve of the tumor is shown in Fig. 1. No significant body weight difference among the groups ($P = 0.300$ and $P = 0.724$ in mono-drug therapy groups; $P = 0.119$, $P = 0.945$, and $P = 0.306$ in combined therapy groups) was found.

Evaluation of CECs using flow cytometry in mice models

Higher aCEC values were observed in rh-endostatin group on day 4 ($19.19 \pm 1.08/\mu\text{l}$ vs. $18.12 \pm 2.02/\mu\text{l}$, $P = 0.259$), which were significantly high on day 7 ($41.25 \pm 10.91/\mu\text{l}$ vs. $21.43 \pm 3.56/\mu\text{l}$, $P = 0.001$); however, it decreased on day 10 ($20.17 \pm 2.63/\mu\text{l}$ vs. $25.17 \pm 3.91/\mu\text{l}$, $P = 0.026$) and returned to control values on day 16. Apoptotic CECs increased on day 10 in rh-endostatin group ($10.84 \pm 2.00/\mu\text{l}$ vs. $7.18 \pm 2.14/\mu\text{l}$, $P = 0.033$) and returned to control values on day 16 ($P = 0.530$). However, cisplatin alone caused a decreasing tendency for CECs, but without significant difference in aCECs and apoptotic CECs compared with control group (Fig. 2). Both combined group 2 and 3 showed a significant decrease in aCECs compared with control group after treatment on day 28 ($28.20 \pm 3.65/\mu\text{l}$ and $35.28 \pm 7.01/\mu\text{l}$ vs. $51.67 \pm 6.12/\mu\text{l}$, $P = 0.003$ and $P = 0.028$, respectively). All the three combined groups led to a significant increase in apoptotic CECs ($5.99 \pm 0.98/\mu\text{l}$, $8.12 \pm 0.47/\mu\text{l}$ and $6.88 \pm 0.77/\mu\text{l}$ vs. $3.64 \pm 0.27/\mu\text{l}$, $P = 0.000$, $P = 0.000$, and $P = 0.000$, respectively).

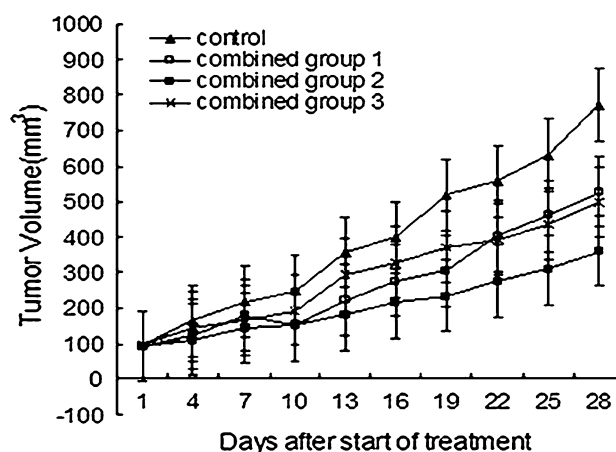
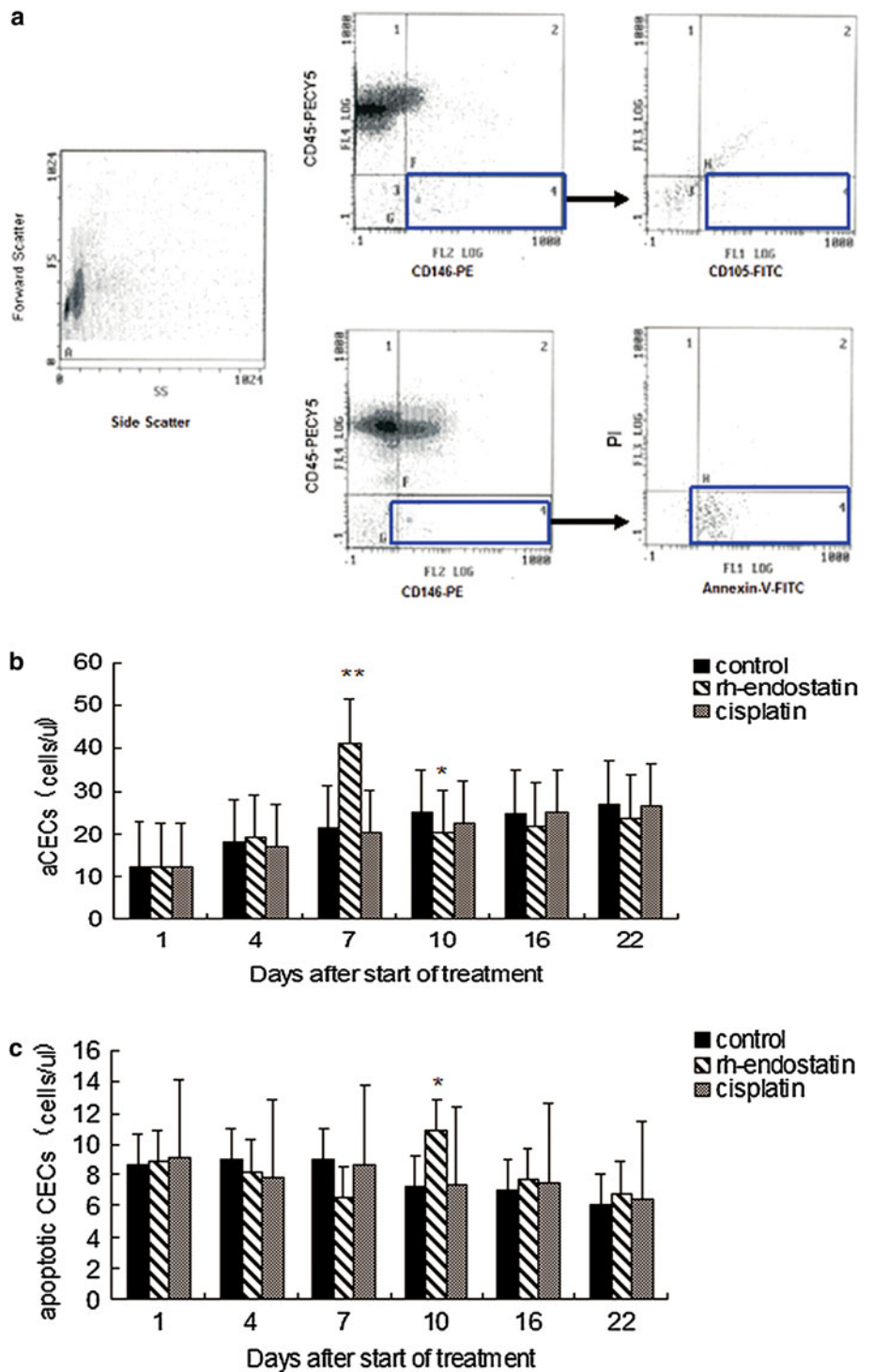


Fig. 1 The growth curve of A549 lung adenocarcinoma in different combined therapy groups. All the three combined groups significantly inhibited the tumor growth compared with control group ($P = 0.010$, $P = 0.000$, and $P = 0.000$ respectively), and the rh-endostatin given first followed by cisplatin group provided more effective anti-tumor activity than the other combined groups

Fig. 2 Validation of viable and apoptotic CEC enumeration. **a** *Left panel* shows the gate used to exclude platelets, dead cells, and debris. Enumeration of aCECs depicted as CD45⁻CD146⁺CD105⁺ cells (*right top panel*), and enumeration of apoptotic CECs depicted as CD45⁻CD146⁺Annexin V⁺PI⁻ cells (*right bottom panel*). **b** Quantification of aCECs at indicated days. **c** Quantification of apoptotic CECs at indicated days. **P* < 0.05; ***P* < 0.01

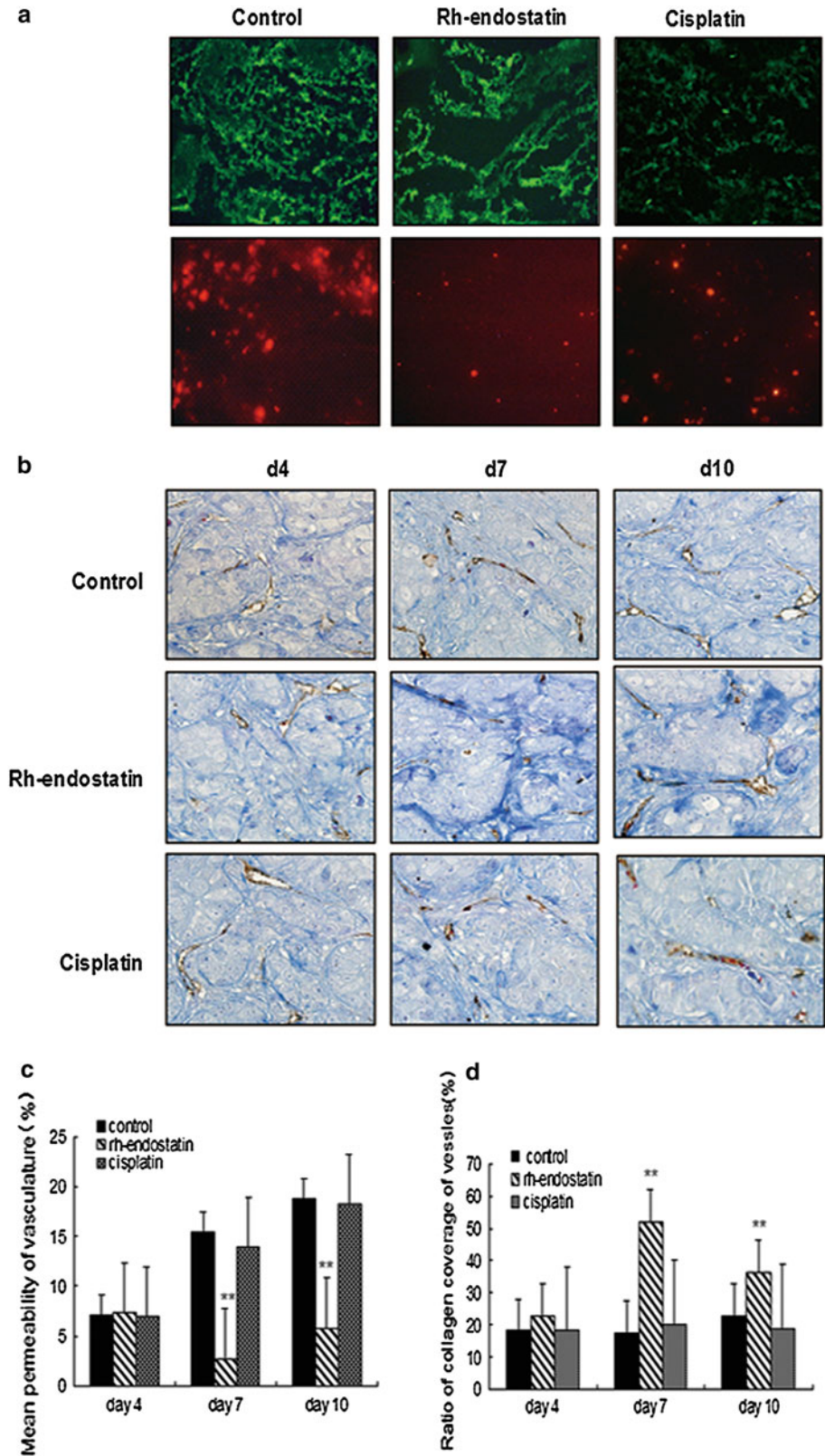


Tumor vascular permeability decreased by rh-endostatin

Tumor vessels in control group revealed tortuous morphology, dilation, and multibranch bifurcation with more TRITC-dextran released from the vessels on days 7 and 10 (15.42 ± 2.49 % and 18.85 ± 1.63 %, respectively). Compared with control group, the tumor vasculature in rh-

endostatin group had fewer giant branches and blood vessel tortuosity, together with decreased dilation, which significantly alleviated vascular permeability (2.69 ± 0.53 % and 5.79 ± 0.92 % on days 7 and 10, *P* = 0.000 and *P* = 0.000, respectively) (Fig. 3a). However, the vasculature became abnormal again, and vascular permeability levels had returned to control values 16 days after therapy (*P* = 0.548).

Fig. 3 Vascular morphology and function improved by rh-endostatin. **a** Representative photographs of tumor vessels on the 7th day after rh-endostatin administration. *Green*, the tumor vasculatures were stained with FITC-lectin; *red*, vascular permeability was represented by the diffused TRITC-dextran. **b** Representative Masson's trichrome staining of tumor vessels. **c** Vascular permeability and **d** ratio of collagen coverage of vessels were quantified in 10 random fields at $\times 400$ magnification, and values at indicated days after rh-endostatin administration were shown. $*P < 0.05$; $**P < 0.01$



Inhibitory effect of rh-endostatin on MVD

After rh-endostatin administration on days 4, 7, 10, and 16, the tumor MVD was 9.67 ± 1.91 , 4.73 ± 1.33 , 10.73 ± 1.91 , and 15.67 ± 2.06 , respectively; the tumor MVD in control group was 10.6 ± 1.99 , 12.40 ± 1.50 , 15.80 ± 4.36 , and 18.20 ± 2.78 on the same time points, and the difference had reached statistical significance on days 7 and 10 ($P = 0.000$ and $P = 0.001$, respectively) (Fig. 4). After treatment on day 28, MVD in three combined groups was significantly decreased (22.40 ± 6.85 , 18.27 ± 2.58 , and 23.87 ± 4.58 vs. 29.73 ± 5.84 , $P = 0.023$, $P = 0.000$, and $P = 0.029$, respectively).

The collagen coverage of tumor vasculature increased by rh-endostatin

After rh-endostatin administration on days 4, 7, 10, and 16, the ratio of collagen coverage of vessels was $22.67 \pm 8.03\%$, $51.83 \pm 14.09\%$, $36.14 \pm 12.56\%$, and $24.96 \pm 5.91\%$ with the ratio in control group was $18.05 \pm 7.08\%$, $17.49 \pm 4.26\%$, $22.54 \pm 11.06\%$, and $20.39 \pm 7.94\%$ on the time points. The difference had reached statistical significance on days 7 and 10 ($P = 0.000$ and $P = 0.002$, respectively) (Fig. 3b, c). After treatment on day 28, the ratio in the three combined groups was significantly increased ($23.57 \pm 4.34\%$, $25.10 \pm 5.18\%$, and $24.16 \pm 4.43\%$ vs. $19.08 \pm 7.07\%$, $P = 0.026$, $P = 0.003$, and $P = 0.012$, respectively).

Tumor hypoxia decreased by rh-endostatin

A significant decrease in hypoxia-inducible factor-1 α (HIF-1 α) was observed in rh-endostatin group on day 7 compared with control group ($28.24 \times 10^4 \pm 3.75 \times 10^4$ vs. $42.11 \times 10^4 \pm 4.35 \times 10^4$, $P = 0.000$). However, it had returned to control values ($39.89 \times 10^4 \pm 2.97 \times 10^4$ vs. $41.49 \times 10^4 \pm 3.40 \times 10^4$, $P = 0.071$) 10 days after therapy (Fig. 5b, c). After treatment on day 28, a significant decrease in HIF-1 α was observed in combined group 2 and 3 compared with control group ($35.71 \times 10^4 \pm 4.56 \times 10^4$ and $37.32 \times 10^4 \pm 3.46 \times 10^4$ vs. $42.34 \times 10^4 \pm 2.72 \times 10^4$, $P = 0.000$, and $P = 0.000$, respectively). No significant difference was found between combined group 1 and control group ($40.58 \times 10^4 \pm 3.43 \times 10^4$ vs. $42.34 \times 10^4 \pm 2.72 \times 10^4$, $P = 0.599$).

Pro-angiogenesis factors down-regulated by rh-endostatin

After rh-endostatin monotherapy, pro-angiogenesis factors, such as EMMPRIN, VEGF, MMP-2, and MMP-9, decreased markedly on day 4 compared with control group

($31.22 \times 10^4 \pm 4.84 \times 10^4$ vs. $39.48 \times 10^4 \pm 2.83 \times 10^4$, $21.52 \times 10^4 \pm 3.51 \times 10^4$ vs. $40.59 \times 10^4 \pm 4.33 \times 10^4$, $24.56 \times 10^4 \pm 7.92 \times 10^4$ vs. $37.77 \times 10^4 \pm 4.46 \times 10^4$, and $19.64 \times 10^4 \pm 6.60 \times 10^4$ vs. $40.87 \times 10^4 \pm 4.27 \times 10^4$, $P = 0.000$, $P = 0.000$, $P = 0.001$, and $P = 0.000$, respectively) (Figs. 5a, c, 6a, c). EMMPRIN increased again on day 16 ($52.18 \times 10^4 \pm 3.61 \times 10^4$ vs. $54.25 \times 10^4 \pm 4.84 \times 10^4$, $P = 0.081$), whereas VEGF and MMP-9 increased again on day 10 ($39.99 \times 10^4 \pm 5.43 \times 10^4$ vs. $42.57 \times 10^4 \pm 4.36 \times 10^4$, $P = 0.073$, and $42.01 \times 10^4 \pm 3.99 \times 10^4$ vs. $43.37 \times 10^4 \pm 3.07 \times 10^4$, $P = 0.236$, respectively). MMP-2 increased again on day 7 ($37.26 \times 10^4 \pm 3.91 \times 10^4$ vs. $39.72 \times 10^4 \pm 2.61 \times 10^4$, $P = 0.074$). After treatment on day 28, EMMPRIN, VEGF, MMP-2, and MMP-9 in three combined groups were significantly down-regulated (all at $P < 0.05$).

Anti-angiogenesis factors up-regulated by rh-endostatin

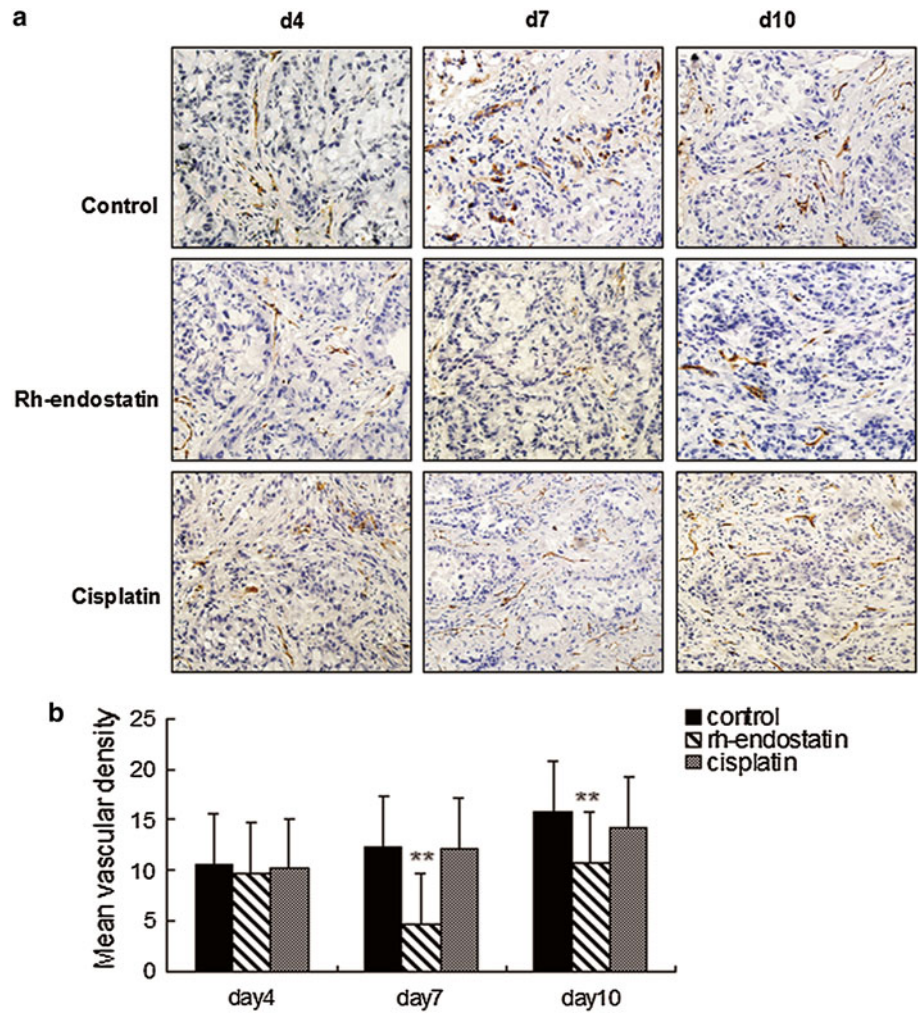
After rh-endostatin monotherapy on days 4, 7, and 10, the IOD of TIMP-1 was $(27.04 \pm 3.57) \times 10^4$, $(28.42 \pm 3.29) \times 10^4$, and $(24.91 \pm 3.66) \times 10^4$ with that in control group was $(22.92 \pm 3.72) \times 10^4$, $(22.93 \pm 5.24) \times 10^4$, and $(23.29 \pm 4.49) \times 10^4$. The difference had reached statistical significance on days 4 and 7 ($P = 0.013$ and $P = 0.001$, respectively) (Fig. 6b, c). On days 4, 7, and 10, the IOD of TIMP-2 in rh-endostatin group was $(24.14 \pm 2.81) \times 10^4$, $(22.98 \pm 2.60) \times 10^4$, and $(21.50 \pm 8.96) \times 10^4$ with that in control group was $(17.79 \pm 7.85) \times 10^4$, $(18.91 \pm 7.36) \times 10^4$, and $(19.76 \pm 4.56) \times 10^4$. The difference had reached statistical significance on days 4 and 7 ($P = 0.025$ and $P = 0.012$, respectively). After treatment on day 28, TIMP-2 in three combined groups were significantly up-regulated, $(22.47 \pm 4.31) \times 10^4$, $(27.08 \pm 3.56) \times 10^4$, and $(21.31 \pm 3.91) \times 10^4$ versus $(16.39 \pm 2.88) \times 10^4$ ($P = 0.000$, $P = 0.001$, and $P = 0.000$, respectively). However, the up-regulation of TIMP-1 was not observed in any combined groups ($P = 0.055$, $P = 0.238$ and $P = 0.772$, respectively).

The correlation among indexes

A positive correlation was found among EMMPRIN, VEGF, MMPs, and MVD, as well as among EMMPRIN, VEGF, MMPs, and HIF-1 α , and it was also found between HIF-1 α and tumor volume. TIMP-1 was negatively correlated with MMP-9 and HIF-1 α . TIMP-2 was also negatively correlated with VEGF, MMP-9, and HIF-1 α . The collagen coverage of vessels was negatively correlated with MVD, VEGF, HIF-1 α , MMP-2, and MMP-9; however, it was positively correlated with TIMP-1 and TIMP-2 (Table 1).

Fig. 4 Time course analyses of tumor microvessel density (MVD) after the initiation of rh-endostatin treatment.

a Representative photographs stained by antibody to CD34 in tumor tissues harvested from five mice in each group killed on days 4, 7, and 10 after treatment initiation. **b** MVD was quantified in 5 random fields at $\times 200$ magnification, and values of MVD at indicated days were shown. $*P < 0.05$; $**P < 0.01$



Discussion

Hypoxia is a common event in solid tumors, and HIF-1 α is considered to be the master regulator involved in sensing and responding to hypoxia, which stimulates the secretion of a number of pro-angiogenesis factors including VEGF, EMMPRIN, and MMPs. VEGF, the predominant factor that stimulates tumor angiogenesis, can not only promote survival and inhibit apoptosis of vascular endothelial cells (Mancuso et al. 2003), but also stimulate secretion of MMPs (Wagner et al. 2003). MMPs, especially MMP-2 and MMP-9, are known to be crucial for degrading type IV collagen of the basement membranes, increasing vascular leakiness, and increasing interstitial fluid pressure (IFP) (Zucker and Vacirca 2004). MMPs are enhanced by EMMPRIN and antagonized by TIMPs (Reimers et al. 2004).

The imbalance of pro- and anti-angiogenesis factors is considered responsible for tumor vascular abnormalities, representing an increased MVD and incomplete pericyte and endothelial coverage (Carmeliet and Jain 2000). Such

abnormalities lead to perfusion obstruction, high leakiness, increased IFP on micrangium around the tumor and blood turbulence, and thereby impeding the oxygen delivery and perfusion of cytotoxic agents to intratumoral sites. This vicious cycle further exacerbates tumor hypoxia, increasing the resistance of tumor cells to chemotherapy. Thus, returning the abnormal state to normalcy may be one of the main targets of anti-angiogenesis therapy to reinforce chemotherapeutic efficacy. Huang and Chen (2010) found that rh-endostatin could normalize tumor vasculature and microenvironment in Lewis lung carcinoma tumor, and during the time of vascular normalization, paclitaxel treatment was found to have maximal effect on tumor growth delay. In contrast, other researchers proposed that the normalization is transient and less effective, thereby cytotoxic drugs should be given earlier to reduce the tumor burden and, subsequently, reducing the secretion of angiogenesis factors, which increases the sensitivity of angiogenesis inhibitors. Recently, avastin treatment combined with chemotherapeutic drugs of the latter model on lung cancer achieved satisfactory results (Ramalingam et al.

Fig. 5 Time course analyses of VEGF and HIF-1 α after the initiation of rh-endostatin treatment. **a** Representative photographs stained by antibody to VEGF in tumor tissues harvested from five mice in each group killed on days 4, 7, and 10. **b** Representative photographs stained by antibody to HIF-1 α on days 4, 7, and 10. **c** VEGF and HIF-1 α were quantified in 10 random fields at $\times 400$ magnification, and values at indicated days were shown. * $P < 0.05$; ** $P < 0.01$

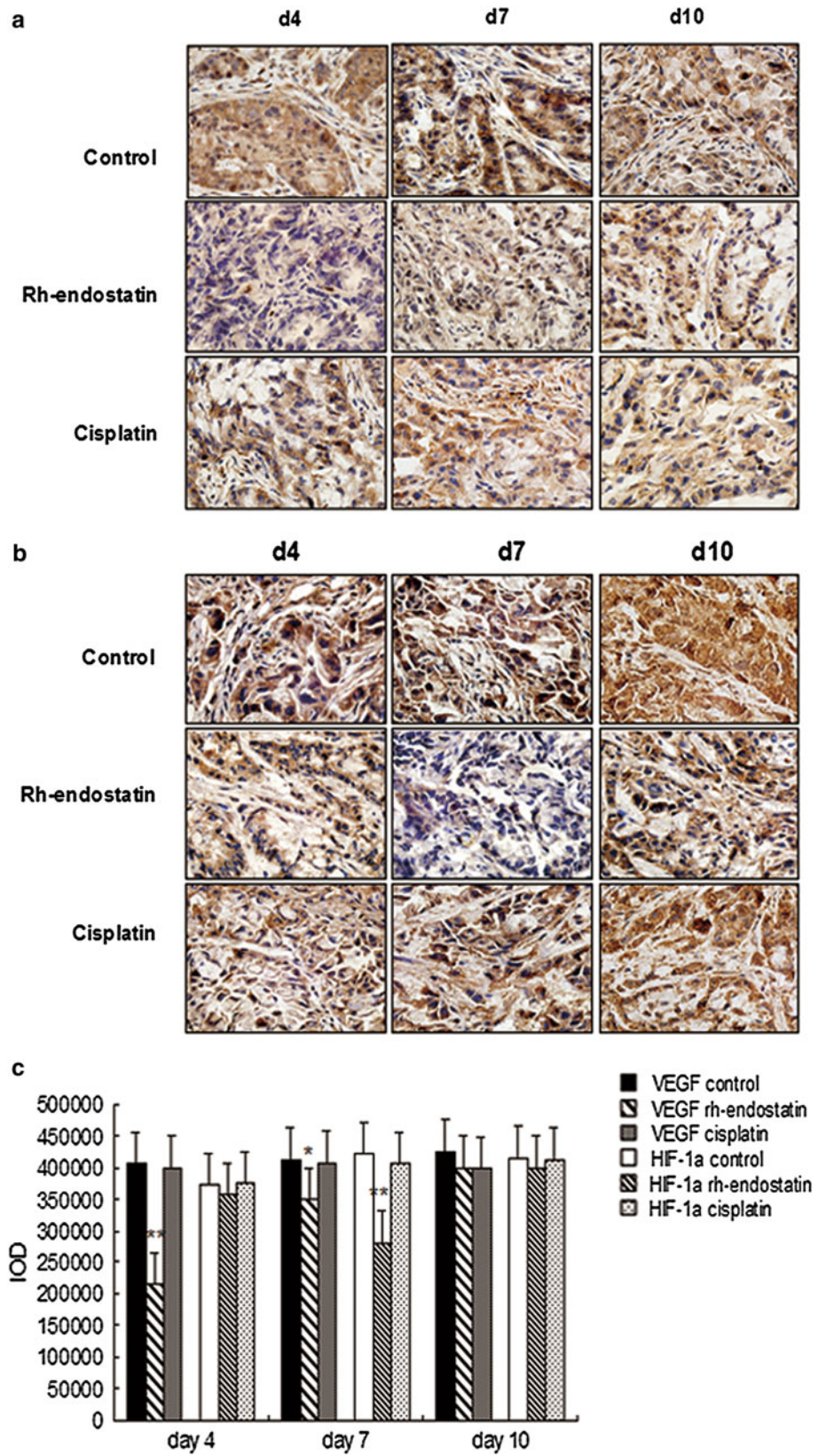
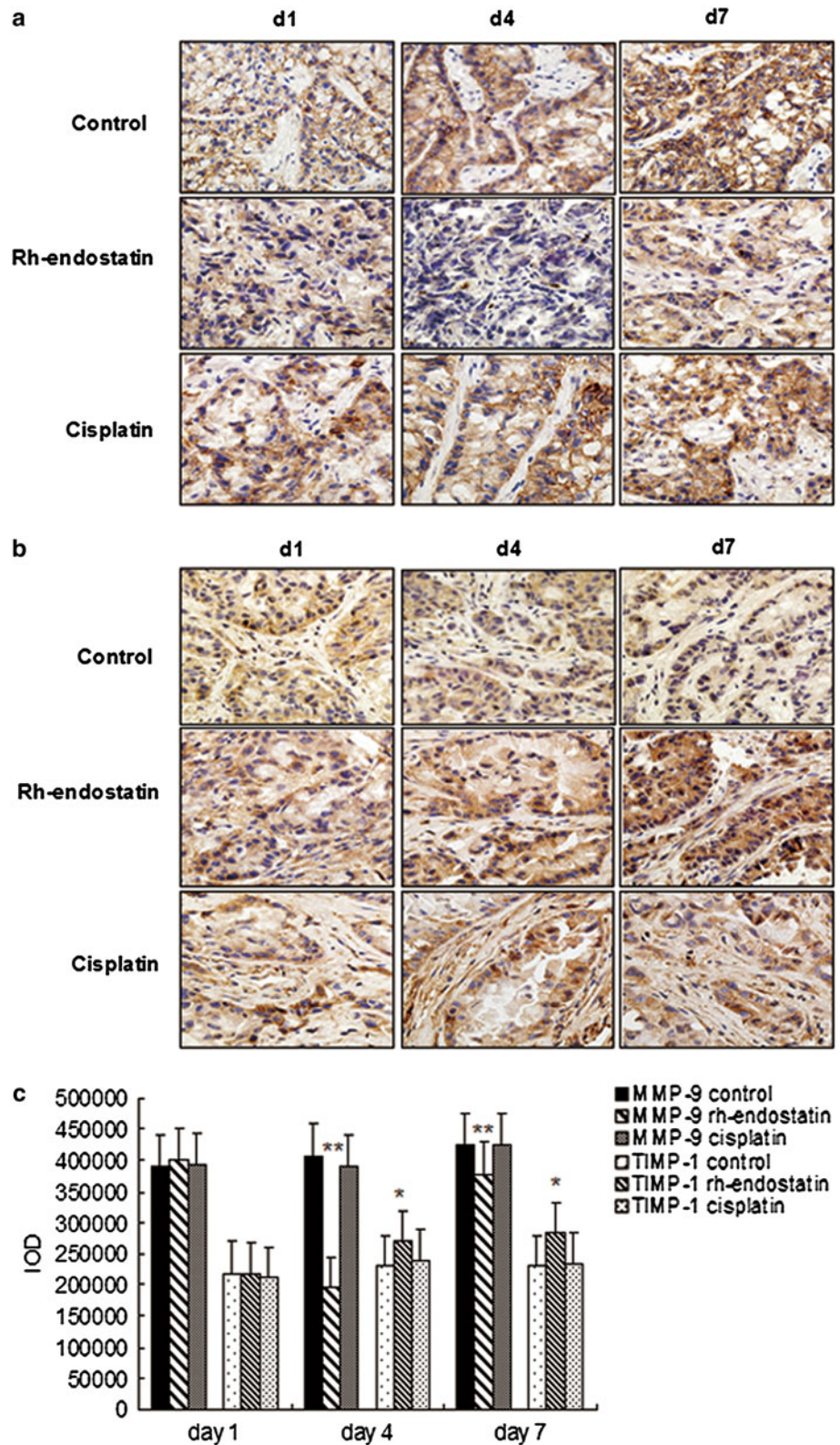


Fig. 6 Time course analyses of MMP-9 and TIMP-1 after the initiation of rh-endostatin treatment. **a** Representative photographs stained by antibody to MMP-9 in tumor tissues harvested from five mice in each group killed on days 1, 4, and 7. **b** Representative photographs stained by antibody to TIMP-1 on days 1, 4, and 7. **c** MMP-9 and TIMP-1 were quantified in 10 random fields at $\times 400$ magnification, and values at indicated days were shown. $*P < 0.05$; $**P < 0.01$



2008). Therefore, an urgent study should be conducted to compare the efficacy of the two therapeutic schedules to determine the optimum treatment.

Endostatin, a 20-kDa hydrolyzed segment of the carboxyl terminal of collagen XVIII, was capable of inhibiting endothelial cell proliferation and migration and inducing

Table 1 The relationship between angiogenesis-related factors and MVD

	MVD	VEGF	MMP-2	MMP-9	EMMPRIN	TIMP-1	TIMP-2	HIF-1 α	Collagen coverage
MVD									
<i>r</i>	1.000	0.446	0.507	0.441	0.478	0.182	0.058	0.093	−0.302
<i>P</i>	–	0.000	0.000	0.000	0.000	0.086	0.589	0.382	0.004
VEGF									
<i>r</i>	0.446	1.000	0.674	0.531	0.780	−0.109	−0.163	0.390	−0.272
<i>P</i>	0.000	–	0.000	0.000	0.000	0.185	0.046	0.000	0.009
MMP-2									
<i>r</i>	0.507	0.674	1.000	0.409	0.629	0.006	−0.073	0.314	−0.356
<i>P</i>	0.000	0.000	–	0.000	0.000	0.941	0.378	0.000	0.001
MMP-9									
<i>r</i>	0.441	0.531	0.409	1.000	0.380	−0.165	−0.194	0.280	−0.328
<i>P</i>	0.000	0.000	0.000	–	0.000	0.044	0.018	0.001	0.002
EMMPRIN									
<i>r</i>	0.478	0.780	0.629	0.380	1.000	0.003	0.009	0.373	0.045
<i>P</i>	0.000	0.000	0.000	0.000	–	0.973	0.908	0.000	0.676
TIMP-1									
<i>r</i>	0.182	−0.109	0.006	−0.165	0.003	1.000	0.132	−0.170	0.401
<i>P</i>	0.086	0.185	0.941	0.044	0.973	–	0.108	0.037	0.000
TIMP-2									
<i>r</i>	0.058	−0.163	−0.073	−0.194	0.009	0.132	1.000	−0.182	0.326
<i>P</i>	0.589	0.046	0.378	0.018	0.908	0.108	–	0.026	0.002
HIF-1α									
<i>r</i>	0.093	0.390	0.314	0.280	0.373	−0.170	−0.182	1.000	−0.245
<i>P</i>	0.382	0.000	0.000	0.001	0.000	0.037	0.026	–	0.020
Collagen coverage									
<i>r</i>	−0.302	−0.272	−0.356	−0.328	0.045	0.401	0.326	−0.245	1.000
<i>P</i>	0.004	0.009	0.001	0.002	0.676	0.000	0.002	0.020	–

endothelial cell apoptosis to inhibit the growth and metastasis of tumor cells through the vessels. Rh-endostatin, a novel recombinant humanized endostatin, was purified in an *Escherichia coli* system with an additional nine amino acid sequence of soluble protein, which improved the stability of the protein. In a phase III clinical trial of rh-endostatin in China, the combination of rh-endostatin and chemotherapy was demonstrated to significantly improve the overall and progression-free survival of advanced non-small-cell lung cancer (Wang et al. 2005). In the present study, single rh-endostatin exhibited mild anti-tumor effect ($P = 0.013$); however, cisplatin failed to inhibit the tumor growth ($P = 0.167$), which may be because cisplatin was given by the maximum tolerated dose (MTD) instead of the low-dose metronomic (LDM) chemotherapy; although it could inhibit the tumor growth shortly, the tumor volume may re-increase with its termination (Zhen et al. 2010). Therefore, the anti-tumor effects of rh-endostatin combined with cisplatin under different administration sequences were observed. Four days after

rh-endostatin administration, the expression of EMMPRIN, VEGF, MMP-2, and MMP-9 began to decrease with the increased expression of TIMP-1 and TIMP-2. After 7 days of rh-endostatin treatment, the tumor vasculature underwent morphologic normalization, including decreased MVD, blood vessel tortuosity and dilation, increased collagen coverage of blood vessels, decreased vascular permeability, as well as intratumoral hypoxia. However, this effect was transient because the above factors returned almost equal to the control values again 16 days after therapy. In the present study, vascular normalization was found to occur on days 4–10 after rh-endostatin administration. The correlations among angiogenesis-related factors showed that the angiogenesis was mainly related to the up-regulation of pro-angiogenesis factors, whereas the increased collagen coverage of vessels and vascular normalization were not only related to the down-regulation of pro-angiogenesis factors (especially MMPs family), but also to the up-regulation of anti-angiogenesis factors. As a result, the vessels were restored to normality with

decreased IFP, causing a hydrostatic pressure gradient across the vascular wall, which facilitated deeper penetration of drugs into tumors, leading to an enhanced response to chemotherapy (Tong et al. 2004). Weichselbaum (2005) found that a significantly synergic effect was achieved only when radiation therapy was applied on days 4–6 after specific anti-VEGFR2 antibody (DC101) administration. Huang and Chen (2010) also found that on days 3–5 or 6–8 following the treatment of rh-endostatin, combination of paclitaxel significantly inhibited the tumor growth. However, when they were concurrently administered, tumor suppression effects were not observed. Moreover, our previous study suggested that the chemotherapy was ineffective outside this normalization window of time after initiation of rh-endostatin, which may be because the vascular normalization effect had disappeared, reducing the distribution of chemotherapeutics into tumors and thus decreasing the anti-tumor effect (Yuan et al. 2010). Considering the conclusion, we did not repeat such kind of regimen in the present study. As expected, the anti-tumor effect was significantly improved when cisplatin was applied during vascular normalization induced by rh-endostatin on days 5–9 than both cisplatin followed by rh-endostatin and simultaneous treatment in which cisplatin was given daily from day 1 to 5. By the way, in our preliminary dose-elevating pre-experiment, cisplatin was given at 3 mg/kg every other day from day 1 to 14; unfortunately, almost all of the mice could not tolerate the toxicity of long-term injection of cisplatin and died, probably owing to continuous and severe borrow suppression. Taken together, anti-angiogenesis drugs should be administered before chemotherapeutics to induce vascular normalization, thus enhancing drug delivery to the tumor. Apparently, the maximal anti-tumor effect can be achieved only when chemotherapy is initiated within the normalization window. Therefore, identifying the normalization window during anti-angiogenesis would be an essential first step in optimizing the anti-tumor effect of the combined therapy. For this reason, finding accurate and effective surrogate markers to monitor the time length of vascular normalization is of critical importance.

Recently, enumeration of CECs has been used as a non-invasive surrogate biomarker for monitoring tumor angiogenesis. CEC levels were increased in patients with various cancer types compared with the healthy controls and decreased significantly after efficient chemotherapy or surgery (Mancuso et al. 2001; Blann et al. 2005). CEC appears in the PB either due to EPC mobilized and released from the bone marrow in response to vascular injury through cytokines (Lyden et al. 2001) or due to shedding from tumor vessels (Chang et al. 2000). Tumor angiogenesis contributes to the mobilization and recruitment of EPCs from bone marrow into the peripheral circulation and the

differentiation of EPCs to mature CECs and then incorporation into newly formed vessels (Asahara et al. 1999a, b). These cells usually need to be activated by tumor angiogenesis factors (TAFs) so that they can home to tumor sites, adhere to form new tumoral vasculature (Furstenberger et al. 2006). For instance, VEGF is essential for the migration, subsequent differentiation, and mobilization of EPC into circulation for the formation of blood vessels (Asahara et al. 1999a, b). Previous studies showed that endostatin reduces aCEC numbers by inhibiting the induction of EPC mobilization by VEGF and inducing their apoptosis (Schuch et al. 2003). Interestingly, the present study showed that aCECs began to increase on day 4 after rh-endostatin administration and most notably on day 7, but significantly decreased on day 10, which was in close coincidence with the decrease of MMPs and vascular permeability. Meanwhile, apoptotic CECs increased on day 10 and decreased to control levels on day 16. The dynamic changes of CECs were supposed to be related to the transient normalization of vascular morphology. Although the mobilization of EPCs could be reduced by decreasing VEGF on day 4 after rh-endostatin administration, vascular normalization induced by decrease of MMPs would likely cause a shedding of CECs from the regressive tumor vessel bed. The increased number of CECs by vessels remodeling was more than the compensation for the reduction of CEP mobilization. Subsequently, rh-endostatin antagonized the EPC mobilization by VEGF and reduced aCEC numbers by inducing their apoptosis (Schuch et al. 2003) and suppressed pro-angiogenesis factors with cisplatin; thus, on day 28 after combined treatment, significant decreases in aCECs and pro-angiogenesis factors were found with significantly decreased MVD. Taken together, we think that transiently increased aCECs at day 7 by rh-endostatin may reflect remodeling tumor vessels, and the start of normalization and increased apoptotic CECs at day 10 may reflect the decreased capacity of angiogenesis and the close of the vascular normalization window. Therefore, the enumerated changes in CECs could be a biomarker for defining the normalization window. Accordingly, when cisplatin was given during the “window”, a more evident decrease of aCECs accompanied by a more conspicuous increase of apoptotic CECs paralleling apparent tumor depression was found. However, the pro-apoptotic effect induced by rh-endostatin was poor, and the apoptotic CECs levels decreased to control values on day 16 after single rh-endostatin administration.

By literatures, some chemotherapeutic agents must be given additional attention, including cyclophosphamide, paclitaxel, and anthracycline, for their mobilization of EPCs and increase of CECs after treatment (Li et al. 2008; Bertolini 2008; Bertolini et al. 2003; Goon et al. 2006; Shaked et al. 2008). There is a probability that when such cytotoxic drugs are combined with anti-angiogenesis drugs

during the “vascular normalization window”, aCECs may not significantly decrease. Nevertheless, when anti-tumor efficacy is enhanced in the combined therapy, the levels of apoptotic CECs may increase (Mancuso et al. 2001). Furthermore, when such chemotherapeutics are given in combined treatments with drugs that can counteract EPCs mobilization, such as DC101, increase of CECs has no longer been found (Shaked et al. 2008).

In conclusion, the restoration of pro- and anti-angiogenesis balance in tumors by rh-endostatin could normalize tumor vasculature for a transient period; thus, combination with cisplatin treatment during vascular normalization exhibited maximally synergistic effects on tumor growth delay. The measurement of CECs including aCECs and apoptotic CECs seems a useful tool to monitor tumor angiogenesis and to evaluate the efficacy of anti-angiogenesis therapies, as well as to help define the vascular normalization window length and make a rational combination therapy schedule in clinic.

Acknowledgments This work was supported by grants from Tianjin Science & Technology Project (No. 09ZCZDSF04400) and CSCO (Y-X2011-001).

Conflict of interest None.

References

- Al-Dissi AN, Haines DM, Singh B et al (2010) Immunohistochemical expression of vascular endothelial growth factor and vascular endothelial growth factor receptor-2 in canine simple mammary gland adenocarcinomas. *Can Vet J* 51(10):1109–1114
- Asahara T, Masuda H, Takahashi T et al (1999a) Bone marrow origin of endothelial progenitor cells responsible for postnatal vasculogenesis in physiological and pathological neovascularization. *Circ Res* 85:221–228
- Asahara T, Takahashi T, Masuda H et al (1999b) VEGF contributes to postnatal neovascularization by mobilizing bone marrow-derived endothelial progenitor cells. *EMBO J* 18(14):3964–3972
- Batchelor TT, Sorensen AG, di Tomaso E et al (2007) AZD2171, a pan-VEGF receptor tyrosine kinase inhibitor, normalizes tumor vasculature and alleviates edema in glioblastoma patients. *Cancer Cell* 11(1):83–95
- Beaudry P, Force J, Naumov GN et al (2005) Differential effects of vascular endothelial growth factor receptor-2 inhibitor ZD6474 on circulating endothelial progenitors and mature circulating endothelial cells: implications for use as a surrogate marker of antiangiogenic activity. *Clin Cancer Res* 11(9):3514–3522
- Bertolini F (2008) Chemotherapy and the tumor microenvironment: the contribution of circulating endothelial cells. *Cancer Metastasis Rev* 27(1):95–101
- Bertolini F, Paul S, Mancuso P et al (2003) Maximum tolerable dose and low-dose metronomic chemotherapy have opposite effects on the mobilization and viability of circulating endothelial progenitor cells. *Cancer Res* 63(15):4342–4346
- Blann AD, Woywodt A, Bertolini F et al (2005) Circulating endothelial cells: Biomarker of vascular disease. *Thromb Haemost* 93(2):228–235
- Carmeliet P, Jain RK (2000) Angiogenesis in cancer and other diseases. *Nature* 407(6801):249–257
- Chang YS, di Tomaso E, McDonald DM et al (2000) Munn LL. Mosaic blood vessels in tumors: frequency of cancer cells in contact with flowing blood. *Proc Natl Acad Sci USA* 97(26):14608–14613
- Folkman J (1971) Tumor angiogenesis: therapeutic implications. *N Engl J Med* 285(21):1182–1186
- Furstenberger G, von Moos R, Lucas R et al (2006) Circulating endothelial cells and angiogenic serum factors during neoadjuvant chemotherapy of primary breast cancer. *Br J Cancer* 94(4):524–531
- Goon PK, Lip GY, Boos CJ et al (2006) Circulating endothelial cells, endothelial progenitor cells, and endothelial microparticles in cancer. *Neoplasia* 8(2):79–88
- Huang G, Chen L (2010) Recombinant human endostatin improves anti-tumor efficacy of paclitaxel by normalizing tumor vasculature in Lewis lung carcinoma. *J Cancer Res Clin Oncol* 136(8):1201–1211
- Huang Y, Song N, Ding Y et al (2009) Pulmonary vascular destabilization in the premetastatic phase facilitates lung metastasis. *Cancer Res* 69(19):7529–7537
- Jain RK (2005) Normalization of tumor vasculature: an emerging concept in antiangiogenic therapy. *Science* 307(5706):58–62
- Khan SS, Solomon MA, McCoy JP Jr (2005) Detection of circulating endothelial cells and endothelial progenitor cells by flow cytometry. *Cytometry B Clin Cytom* 64(1):1–8
- Li H, Raia V, Bertolini F et al (2008) Circulating endothelial cells as a therapeutic marker for thalidomide in combined therapy with chemotherapy drugs in a human prostate cancer model. *BJU Int* 101(7):884–888
- Lyden D, Hattori K, Dias S et al (2001) Impaired recruitment of bone-marrow-derived endothelial and hematopoietic precursor cells blocks tumor angiogenesis and growth. *Nat Med* 7(11):1194–1201
- Mancuso P, Burlini A, Pruneri G et al (2001) Resting and activated endothelial cells are increased in the peripheral blood of cancer patients. *Blood* 97(11):3658–3661
- Mancuso P, Calleri A, Cassi C et al (2003) Circulating endothelial cells as a novel marker of angiogenesis. *Adv Exp Med Biol* 522:83–97
- Ramalingam RR, Dahlberg SE, Langer CJ et al (2008) Outcomes for elderly, advanced-stage non small-cell lung cancer patients treated with bevacizumab in combination with carboplatin and paclitaxel: analysis of Eastern Cooperative Oncology Group Trial 4599. *J Clin Oncol* 26(1):60–65
- Reimers N, Zafrakas K, Assmann V et al (2004) Expression of extracellular matrix metalloproteases inducer on micrometastatic and primary mammary carcinoma cells. *Clin Cancer Res* 10(10):3422–3428
- Schuch G, Heymach JV, Nomi M et al (2003) Endostatin inhibits the vascular endothelial growth factor-induced mobilization of endothelial progenitor cells. *Cancer Res* 63(23):8345–8350
- Shaked Y, Henke E, Roodhart JM et al (2008) Rapid chemotherapy-induced acute endothelial progenitor cell mobilization: implications for antiangiogenic drugs as chemosensitizing agents. *Cancer Cell* 14(3):263–273
- Tong RT, Boucher Y, Kozin SV et al (2004) Vascular normalization by vascular endothelial growth factor receptor 2 blockade induces a pressure gradient across the vasculature and improves drug penetration in tumors. *Cancer Res* 64(11):3731–3736
- Wagner S, Fueller T, Hummel V et al (2003) Influence of VEGFR2 inhibition on MMP secretion and motility of microvascular human cerebral endothelial cells (HCEC). *J Neurooncol* 62(3):221–231
- Wang J, Sun Y, Liu Y et al (2005) Results of randomized, multicenter, double-blind phase III trial of rh-endostatin (YH-

- 16) in treatment of advanced non-small cell lung cancer patients. *Zhongguo Fei Ai Za Zhi* 8(4):283–290
- Weichselbaum RR (2005) How does antiangiogenic therapy affect brain tumor response to radiation? *Nat Clin Pract Oncol* 2(5):232–233
- Weidner N (1995) Intratumor microvessel density as a prognostic factor in cancer. *Am J Pathol* 147(1):9–19
- Yuan J, Wu CW, Liu ZJ et al (2010) Observation of the antitumor effect of endostar combined with docetaxel under different administration sequences. *Chin J Oncol* 32(8):580–585
- Zhen FS, Wang J, Liang J et al (2010) Low-dose metronomic chemotherapy with cisplatin: can it suppress angiogenesis in H22 hepatocarcinoma cells? *Int J Exp Path* 91:10–16
- Zucker S, Vacirca J (2004) Role of matrix metalloproteinases (MMPs) in colorectal cancer. *Cancer Metastasis Rev* 23(1–2): 101–117